Institute of Mechanical Sciences and Industrial Applications

Wind Turbine Noise : current research topics related to wind turbine noise propagation

Benjamin Cotté

Institute of Mechanical Sciences and Industrial Applications (IMSIA)
ENSTA ParisTech, University Paris-Saclay
benjamin.cotte@ensta.fr

CeLyA Summer School Atmospheric sound propagation – 15 June 2018

Short presentation

- PhD student at École Centrale de Lyon under the supervision of Ph. Blanc-Benon, and in collaboration with SNCF (2005–2008)

- Assistant professor at ENSTA ParisTech since 2011: `www.ensta-paristech.fr/~cotte/`

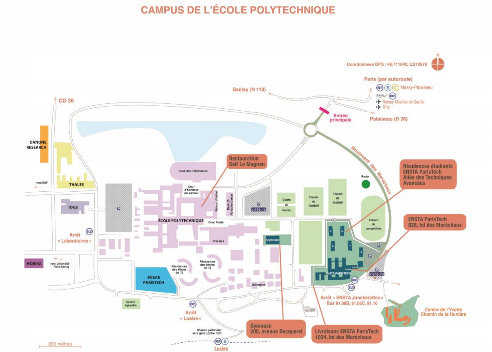

Short presentation

- coordinator with Xavier Boutillon (Polytechnique) of the M2 Acoustical Engineering of the Paris-Saclay University:

https://acoustics-saclay.ensta-paristech.fr

- research activities at IMSIA (UMR EDF-ENSTA-CNRS-CEA)
  - aero- and hydro-acoustics
  - acoustic propagation in the atmosphere
  - structural and musical acoustics

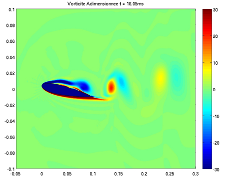

Vorticity field calculated with Code_Safari (Rigall, 2017)

Opus 102 piano designed and built by Stephen Paulello – Development of a sound CAD tool for piano soundboards in the ANR project MAESSTRO

Outline

Wind Energy development

Total installed capacity of 539 GW at the end of 2017:

- 188 GW in China
- 89 GW in the USA
- 56 GW in Germany
- 14 GW in France (7th rank)

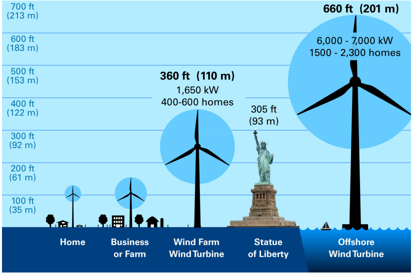

http://www.windenergy.org.nz

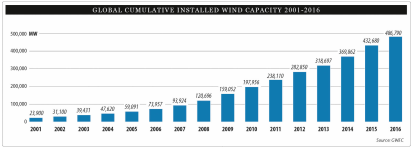

http://energyclassroom.com

Types of wind turbines

- Horizontal Axis Wind Turbines (HAWT) and Vertical Axis Wind Turbines (VAWT)

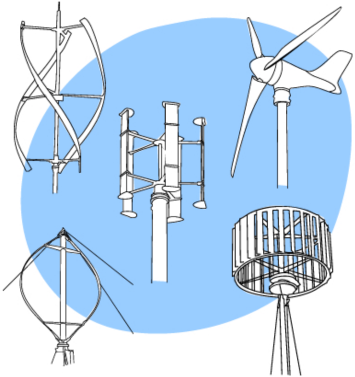

http://www.build.com.au/

- Pitch-regulated and stall-regulated WTs

Typical power curves
(Mihet-Popa and Groza, 2010)

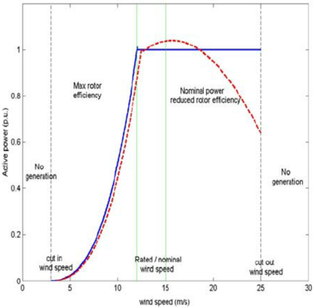

The majority of modern wind turbines are upwind pitch-regulated HAWTs

Wind turbine noise emission

Emission characterized by the sound power level (SWL)

Typical SWL spectrum for a 300 kW stall-regulated WT (Zhu *et al.*, 2005)

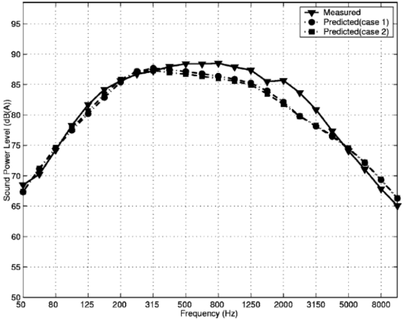

Typical overall SWL evolution with hub height wind speed *U* for a 2.3 MW pitch-regulated WT (Cotté and Tian, 2015)

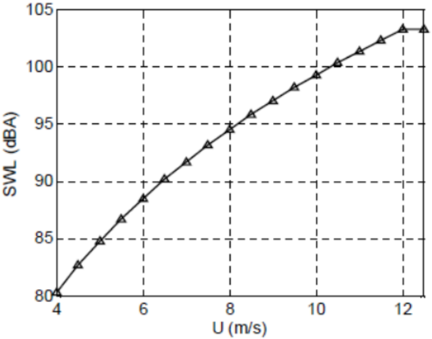

Wind turbine noise directivity

Experimental characterization of Buck *et al.* (2016)

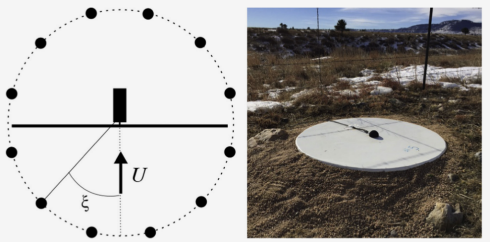

Measurement system: microphone with windscreen placed on a rigid board on the ground with sand edge treatment

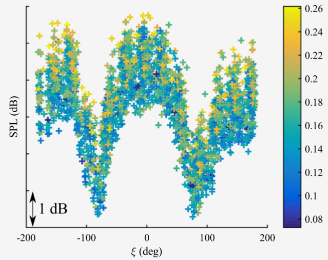

Horizontal directivity of OASPL in dB(A) for wind speeds between 9.0 and 11.5 m/s

Amplitude modulation of wind turbine noise

- Wind turbine noise is characterized by amplitude modulation at the blade passage frequency (BPF), of period ≈ 1 s
- Audible close to the wind turbine in some directions (*normal AM*), and sometimes at larger distances in some environmental conditions (*other AM* or *enhanced AM*). See Oerlemans (2013).

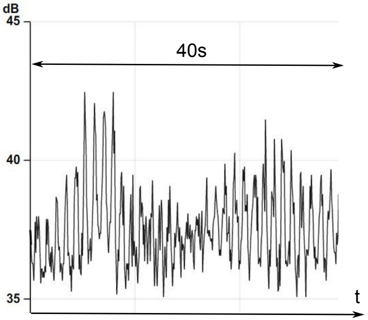

wind turbine measurement in Wadlow (UK) by MAS environmental (`www.masenv.co.uk`)

Amplitude modulation of wind turbine noise

Example of amplitude modulation measured by Dick Bowdler (`www.dickbowdler.co.uk`) 50 m upwind of a 93 m diameter WT

play stop

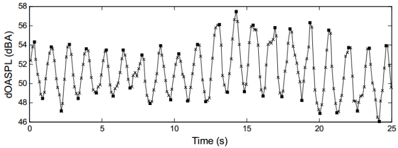

Spectrogram of this measurement (Smith *et al.*, 2012)

Transition from “normal swish” to “thump”

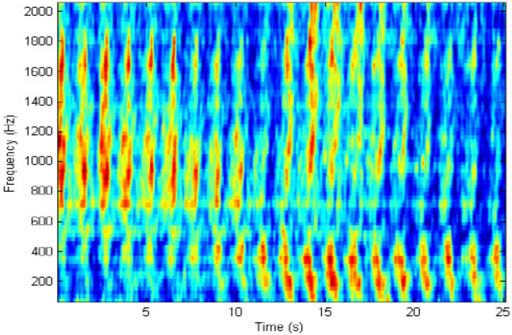

Offshore wind turbine noise

- larger WTs and larger propagation distances

  ⇒ less likely to be heard during operation
- construction noise (piling noise) can potentially be an issue because quite loud

Numerical simulations by Van Renterghem *et al.* (2014)

Sound scattering by a rough sea surface

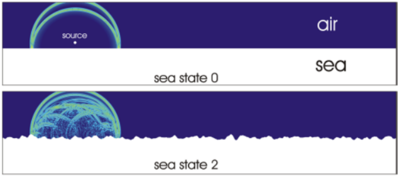

Piling noise SWL spectrum

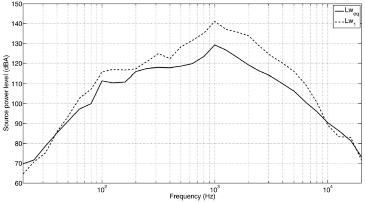

SPL predictions in a neutral atmosphere

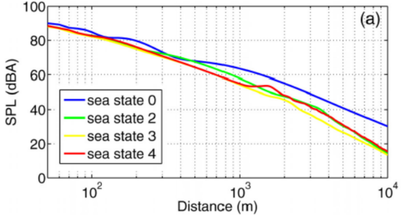

Low frequency noise and infrasound

Downwind WTs in the 80s produced intense low-frequency sound due to the interaction between the tower wake and the blades (Shepherd and Hubbard, 1991)

2 blades – Diameter 61 m

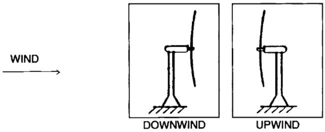

MOD-1 WT

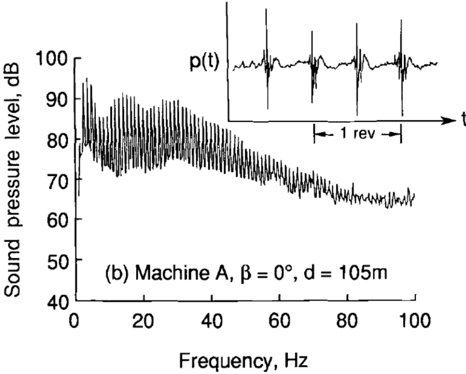

Low-frequency content much reduced with upwind WTs

Low frequency noise and infrasound

Indoor/outdoor power spectral densities measured by Zajamsek *et al.* (2016)
3 km away from the nearest wind turbine

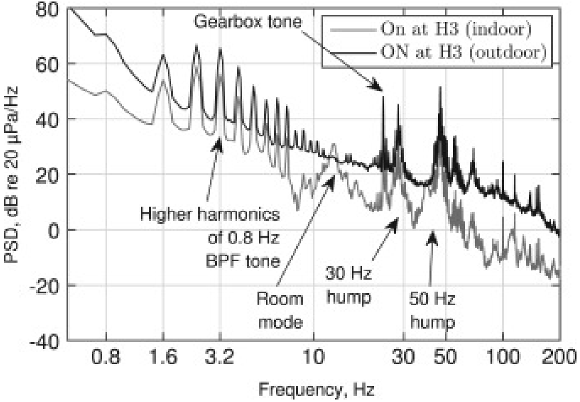

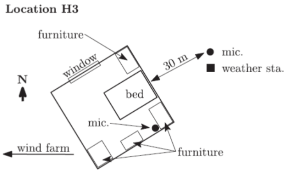

Low frequency noise and infrasound

Experimental characterization of Zajamsek *et al.* (2016)

Relation between the presence of infrasound (criterion based on 4th BPF) and atmospheric stability

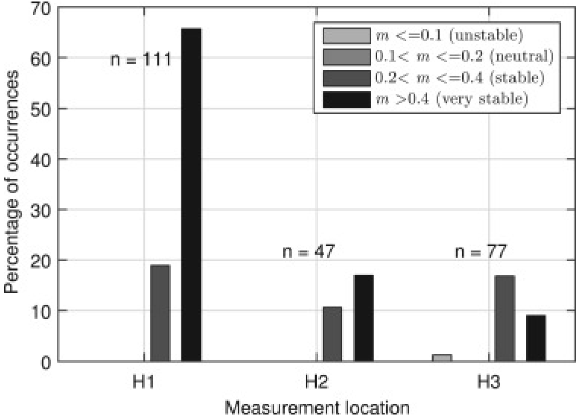

SODAR wind speed profiles

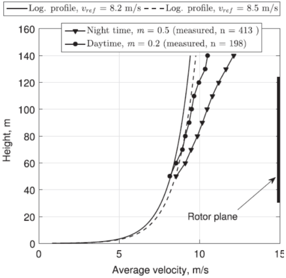

Perception of wind turbine noise

- wind turbine noise can be perceived at large distances (several kilometers)
- low-frequency components (20 Hz $\lesssim f \lesssim$ 200 Hz) dominate at large distances, but no clear proof than infrasound ($f <$ 20 Hz) can be perceived

Low-frequency measurements of Zajamsek *et al.* (2016) at 4 km from a wind farm

Comparison of rms values (10 minutes) to hearing threshold (ISO 226-2003)

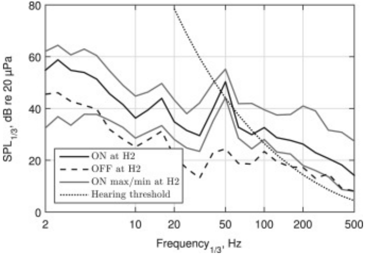

Comparison of peak (1 second) and rms (10 minutes) values to Outer Hair Cell threshold given by Salt and Hullar (2010)

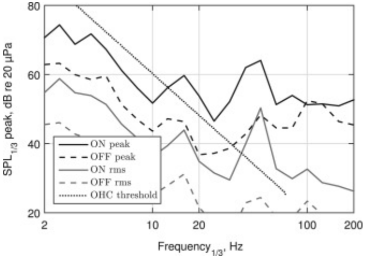

Annoyance related to wind turbine noise

- Results of dose response studies: annoyance is quite high compared to transportation noise (Pedersen and Waye, 2014).
- Could be due to:
  - other factors that play a role, such as the visual impact
  - wind turbine characteristics: amplitude modulation, low background noise in rural area
  - inaccurate estimates of sound exposures at dwellings (Old and Kaliski, 2017)

Pedersen and Waye (2014)

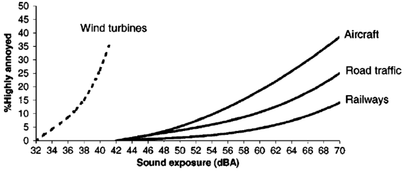

Sound exposure is for wind turbines calculated A-weighted L_{eq} for a hypothetical time period and for transportation DNL.

Old and Kaliski (2017)

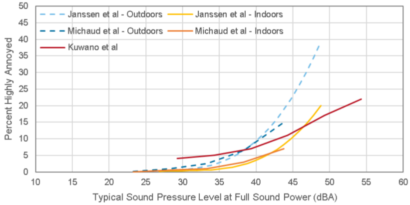

Wind turbine noise regulations

Two main types of regulations depending on the countries:

- based on absolute levels
  e.g. in Denmark: threshold levels of 44 dB(A) for dwellings in open country and 39 dB(A) for other dwellings ($v_{10} = 8$ m/s)
- based on emergence criteria: increase with respect to ambient noise
  e.g. in France: emergence smaller than 5 dB(A) during the day, and 3 dB(A) during the night

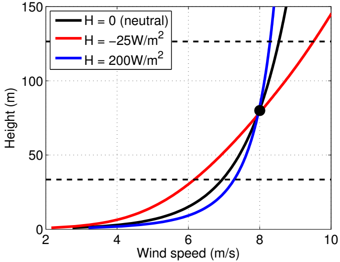

Examples of wind speed profiles

Emergence criteria might be difficult to meet at night for stable atmospheres (strong wind shear)

Outline

Main wind turbine noise sources

- mechanical noise (gearbox)

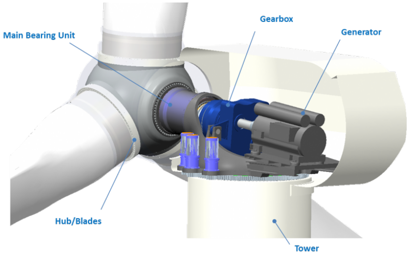

www.eolotec.com

- tonal aeroacoustic noise at BPF and harmonics (e.g. blade-tower interaction noise)

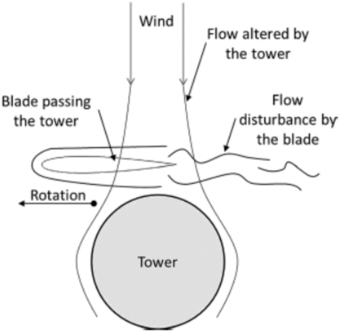

Yauwenas *et al.* (2017)

Main wind turbine noise sources

- broadband aeroacoustic sources
  - turbulent inflow noise
  - turbulent boundary layer trailing edge noise
  - separation/stall noise

⇒ could be the cause of enhanced amplitude modulations (Oerlemans, 2013)

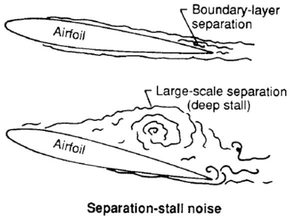

Brooks, Pope and Marcolini (1989)

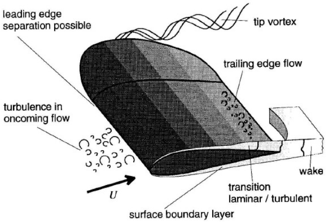

Wagner (1996)

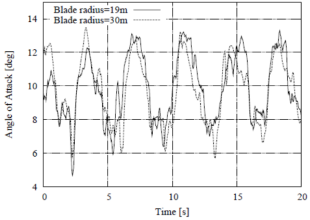

Bertagnolio *et al.* (2015)

Relative importance of TEN and TIN

Experimental characterization of Buck *et al.* (2016) for wind speeds between 9.0 and 11.5 m/s

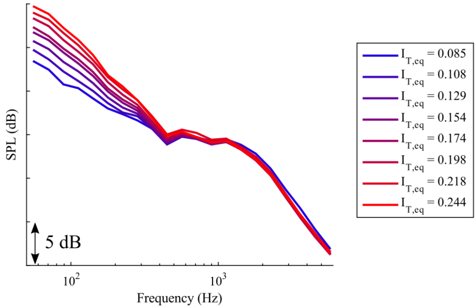

Low-frequency components increase with the “equivalent turbulence intensity” $I_{T,eq}$ esimated on 15-s data segment

$\Rightarrow$ turbulent inflow noise dominates at frequencies below 200-300 Hz while trailing edge noise dominates above

Aeroacoustic source models

Main types of models

1. Semi-empirical models
   Example : BPM model based on experimental database of Brooks, Pope and Marcolini (1989)
   $\Rightarrow$ implemented in NREL Airfoil Noise code within the FAST modular framework.
2. Analytical models:
   Examples : Amiet (1975, 1976), Howe (1978, 1999), ...
3. Computational aeroacoustics
   Example : hybrid approach with:
   - a Large Eddy Simulation (LES) to calculate the flow
   - an acoustic analogy to obtain the far-field radiated noise

Semi-empirical models

Calculations of Barlas *et al.* (JASA 2017) for NREL 5MW reference WT (RD 126 m) at 2 RD downwind

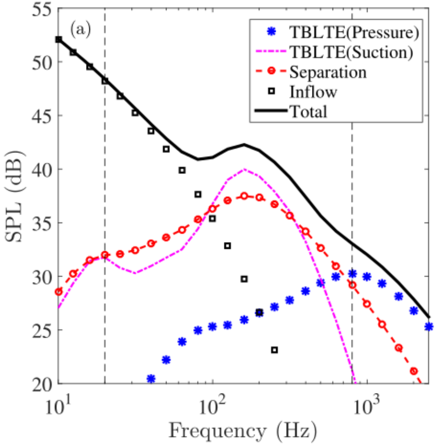

Semi-empirical models

Wind turbine noise directivity: sound pressure level on the ground averaged over one rotation (Zhu *et al.* , 2005)

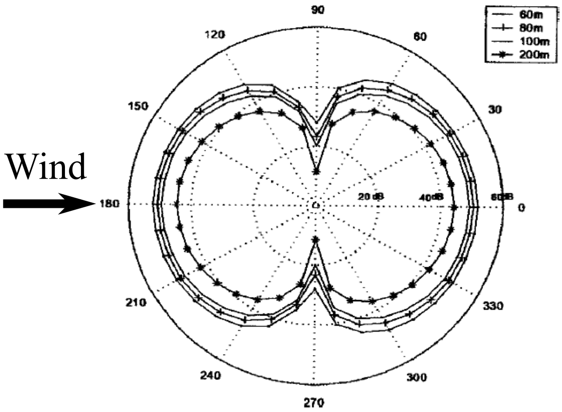

Amiet theory for a fixed airfoil

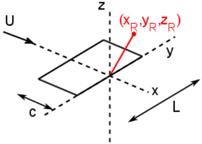

PSD of acoustic pressure calculated for $L/c > 3$

$$S_{pp}^{F}(\mathbf{x_R},\omega) = A(\mathbf{x_R},\omega)\Pi(\mathbf{x_R},\omega)\left|\mathcal{I}(\mathbf{x_R},\omega)\right|^2$$

$\Pi(\mathbf{x_R},\omega)$: spectrum of turbulent fluctuations
$|\mathcal{I}(\mathbf{x_R},\omega)|^2$: aeroacoustic transfer function that contains the source directivity

Trailing edge noise directivity:

- $f = 16\,\mathrm{Hz}\ (kc = 0.2)$
- $f = 50\ Hz (kc = 0.7)$
- $f = 120\ Hz (kc = 1.8)$
- $f = 500\ Hz (kc = 7.2)$

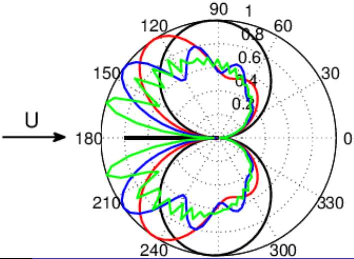

Application to a rotating blade

- each blade is divided into N_s segments (strip theory)
- For each segment at each angular position β:
  - contribution of segment at the receiver calculated using Amiet theory
  - correction due due to Doppler effect

$$S_{pp}^{R}(\mathbf{x_R^T}, \omega, \beta) = \frac{\omega_e}{\omega} S_{pp}^{F}(\mathbf{x_R^B}, \omega_e, \beta)$$

  $\mathbf{x_R^T}$: receiver coordinates in the wind turbine reference system
  $\mathbf{x_R^B}$: receiver coordinates in the blade reference system
  - logarithmic summation

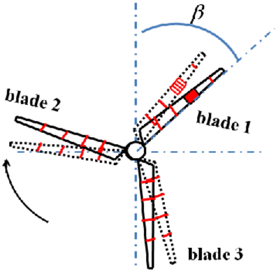

Comparison with 2.3 MW wind turbine measurements

- hub height of 80 m
- rotor diameter of 93 m
- pitch-regulated wind turbine with 3 blades of length 45 m, cut into 8 segments ($L/c > 3$)

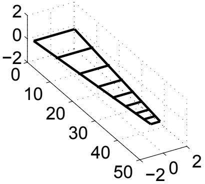

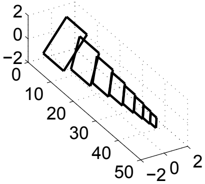

Comparison with 2.3 MW wind turbine measurements

Results of Tian and Cotté (2016)

The measurements are performed at DTU (Leloudas, 2006)

$U_{ref} = 6\,\mathrm{m/s}$ $U_{ref} = 8\,\mathrm{m/s}$

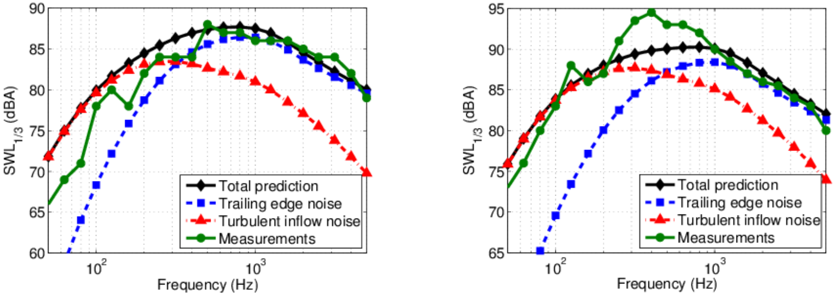

Questions on WTN sources?

Array measurement of Oerlemans *et al.* (2007)

- GAMESA G58 WT at 25 rpm – tip Mach number 0.22
- Array of 148 microphones mounted on a wooden platform
- Measurement time of 30 s and high-pass filtering above 500 Hz

Questions

- What is the effect of the platform on the noise measurements?
- What noise source(s) do you identify?
- Why the dominant sources (red spot) appear during the downward movement of the blades?

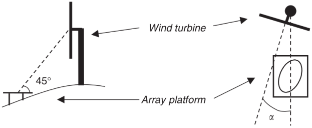

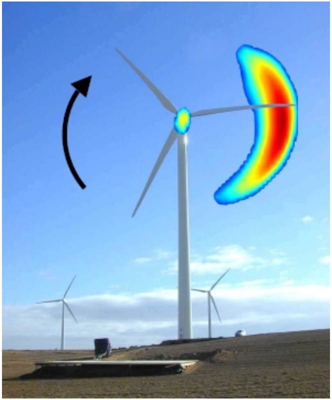

Outline

Wind turbine propagation effects

In this section we focus on the effect of the source modelling with the following simplifications:

- flat and homogeneous ground;
- wake effect neglected;
- simple wind speed and temperature profiles.

From Monin-Obukhov similarity theory for a neutral atmosphere:

$$\bar{u}(z) = \frac{u_*}{\kappa} \ln\left(\frac{z}{z_0}\right)$$

$$\bar{T}(z) = T_0 + \alpha_0 z \quad \text{with} \quad \alpha_0 \approx -0.01\,\text{K/m}$$

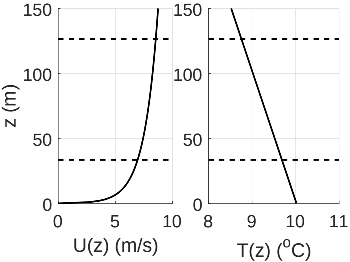

Effective sound speed approximation

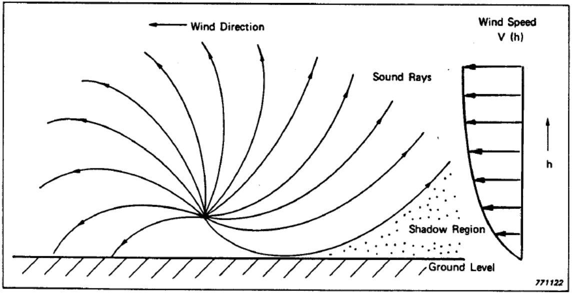

Lamancusa (2009)

Effective sound speed approximation

$$c_{eff}(z) = c(z) + U(z) \cos\theta$$

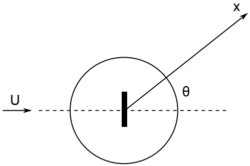

Point source approximation

The wind turbine is represented as a monopole located at hub height

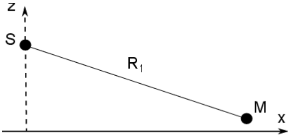

Link between sound power level $L_W(f)$ and sound pressure level $L_p(f)$

$$L_p(f) = L_W(f) - \underbrace{10\log_{10}(4\pi R_1^2)}_{\text{geometrical spreading}} - \underbrace{\alpha(f)R_1}_{\text{atmospheric absorption}} + \underbrace{\Delta L}_{\text{propagation effects}}$$

ΔL can be calculated with any propagation model

Note: this expression is used to estimate the sound power level using a ground microphone on a rigid platform (IEC standard):

$$L_W(f) = L_p(f) + 10\log_{10}(4\pi R_1^2) - 6\,dB + \alpha(f)R_1$$

Point source approximation

Link between sound power level $L_W(f)$ and sound pressure level $L_p(f)$

$$L_p(f) = L_W(f) - 10\log_{10}(4\pi R_1^2) - \alpha(f)R_1 + \Delta L(f)$$

Geometrical spreading

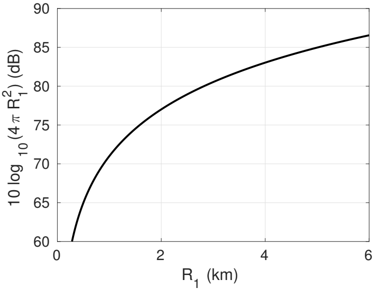

Typical absorption coefficient for a temperature of 10^{o}C and a relative humidity of 80%

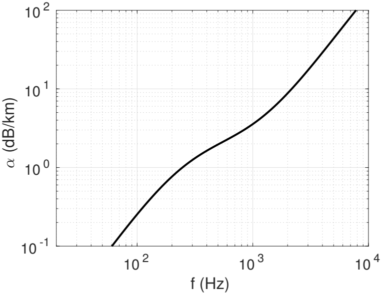

Ray-tracing using the point source approximation

Link between sound power level $L_W(f)$ and sound pressure level $L_p(f)$

$$L_p(f) = L_W(f) - 10\log_{10}(4\pi R_1^2) - \alpha(f)R_1 + \Delta L(f)$$

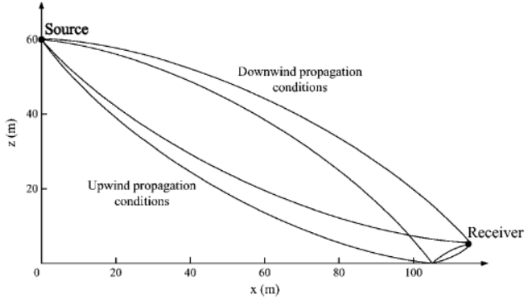

Fig. 13 Downward and upward refraction of eigenrays for downwind and upwind propagation conditions, respectively.

Prospathopoulos and Voutsinas (2005)

Ground effect and point source approximation

Spectra of the level difference between heights of 1.6 m and 0.05 m calculated and measured by Heutschi *et al.* (2014) at distances of 400 m (left) and 250 m (right)

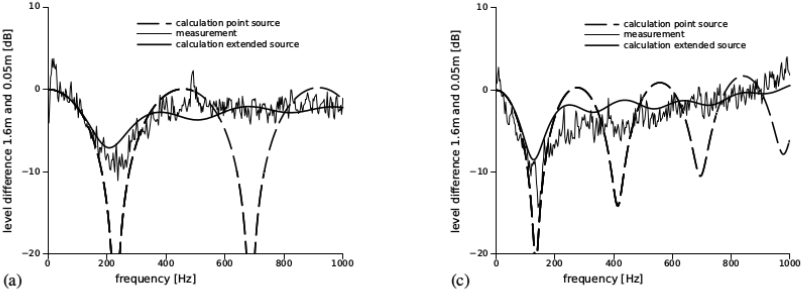

The point source approximation exaggerates the ground interference dips
⇒ need for extended source models

Method 1: backpropagation method in the parabolic approximation (Cotté, 2018)

- axisymmetric approximation of the inhomogeneous Helmholtz equation with $n(z) = c_0/c_{eff}(z)$:

$$\left[\frac{\partial^2}{\partial x^2} + \left(\frac{\partial}{\partial z^2} + k_0^2 n(z)^2\right)\right] q_c = 0 \quad \text{with} \quad q_c = p_c\sqrt{x}$$

- decoupling waves propagating towards $+x$ and $-x$:

$$\left(\frac{\partial}{\partial x} - \gamma i \mathcal{Q}\right) q_\gamma = 0 \quad \text{with} \quad \mathcal{Q} = \left(n(z)^2 + \frac{1}{k_0^2}\frac{\partial}{\partial z^2}\right)^{1/2}$$

$\gamma = +1$: forward-propagation
$\gamma = -1$: back-propagation

- approximation of operator $\mathcal{Q}$: use the Split-Step Padé (N,N) method of Collins (1993) to increase the angular validity and Δx

  $\Rightarrow \Delta x \leq 2\lambda$ with Split-Step Padé (2,2) method

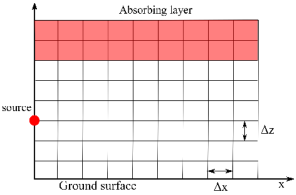

Method 1: backpropagation method in the parabolic approximation (Cotté, 2018)

For each segment and each angular positions:

- numerical starter at $x = 0$ obtained by backpropagating ($\gamma = -1$) a known initial solution from $x = x_{is}$ in homogeneous conditions (Collins, 1991; Dragna, 2011)
- initial solution at $x = x_{is}$ obtained using Amiet's model over a rigid ground:

$$q_c(z_{is,k}) = \sqrt{S_{pp}^R(\mathbf{x}_\mathbf{R}^\mathbf{T}, \omega, \beta)}\sqrt{x_S}\left(e^{ik_0 R_{1,k}} + \frac{R_{1,k}}{R_{2,k}} e^{ik_0 R_{2,k}}\right)$$

- strictly valid only at the receiver at $x = x_R$
- $N_s \times N_\beta$ PE calculations per frequency and per propagation direction

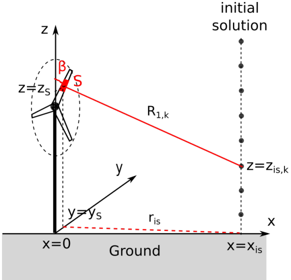

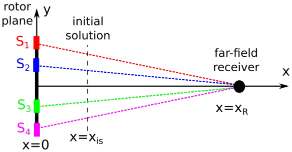

Method 2: moving monopoles model

Point source approximation

For each segment and each angular positions:

$$L_p(f,\beta) = L_W(f,\beta) - 10\log_{10}(4\pi R_1^2) + \Delta L(f) - \alpha(f) R_1$$

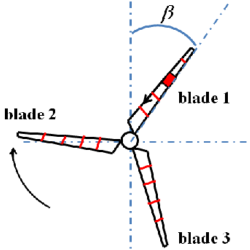

- angle-dependent sound power level $L_W(f,\beta)$ obtained from Amiet model:

$$L_W(f,\beta) = L_{p,FF}(f,\beta) + 10\log_{10}(4\pi R_1^2)$$
$$= 10\log_{10}\left(\frac{S_{pp}^R(\mathbf{x_R^T}, f, \beta)}{p_{\text{ref}}^2}\right) + 10\log_{10}(4\pi R_1^2).$$

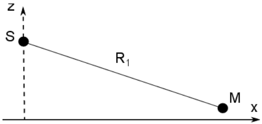

- $\Delta L(f)$ obtained from a set of PE calculations at N_h different heights
  $\Rightarrow$ closest point interpolation based on the segment height at angle β
- N_h PE calculations per frequency and per propagation direction

Validation test cases

- 2.3 MW wind turbine with tower height 80 m
- variable porosity impedance model for a natural ground (Dragna *et al.*, 2015)
- test-case 1: only trailing edge noise and homogeneous conditions ($c(z) = c_0$)

$\Rightarrow$ reference solution based on image source

- test-case 2: both source mechanisms and profiles of $T(z)$ and $U(z)$ in a neutral atmosphere

Calculation parameters:

- 49 frequencies between 100 Hz and 2000 Hz
- domain: 1200 m along x and 300 m along z
- 30 angular positions β
- method 1: initial solution calculated at $x_{is} = 100$ m
- method 2: N_h varied between 1 and 19

Third octave band spectra in homogeneous conditions

spectra at $z = 2\,\mathrm{m}$ and at $x = 500\,\mathrm{m}$ or $x = 1000\,\mathrm{m}$ downwind ($\tau = 0^o$)

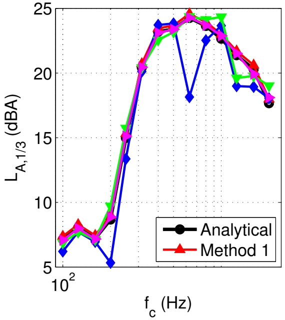

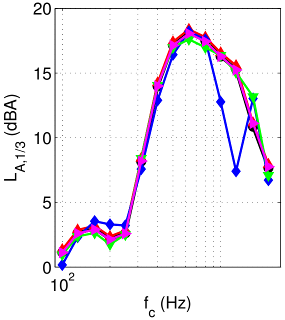

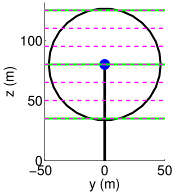

Third octave band spectra in homogeneous conditions

spectra at $z = 2$ m and at $x = 500$ m or $x = 1000$ m crosswind ($\tau = 90^o$)

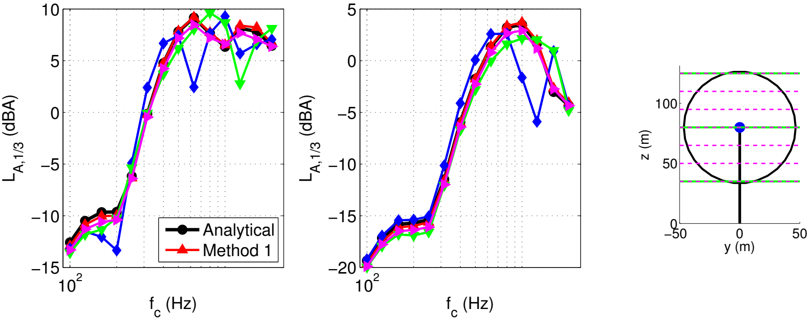

- Excellent results with $N_h = 7$ heights
- Slight underestimation crosswind (0.4-0.5 dB) that can be attributed to directivity effects
- CPU time is $N_s N_\beta / N_h \approx 34$ times smaller with method 2!

Overall SPL and amplitude modulation

Overall SPL averaged over one rotation (OASPL)

Amplitude Modulation : $\mathrm{AM} = \max_{\beta} \mathrm{OASPL}(\beta) - \min_{\beta} \mathrm{OASPL}(\beta)$

OASPL and AM at $z = 2\,\mathrm{m}$ crosswind ($\tau = 90^o$)

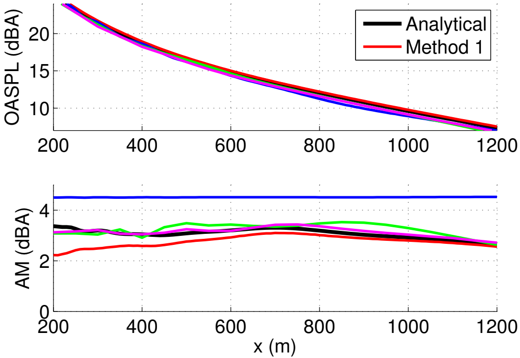

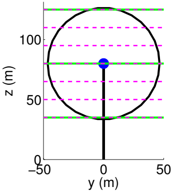

Horizontal directivity of OASPL and AM in homogeneous conditions

Directivity at $x = 1000\,\text{m}$ and $z = 2\,\text{m}$

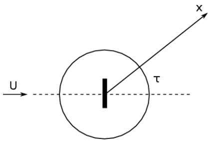

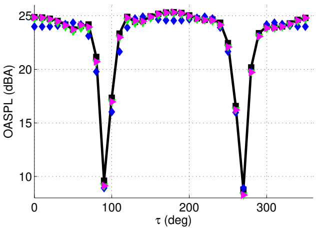

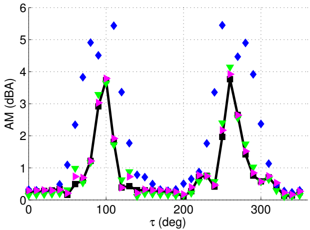

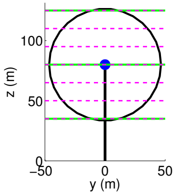

- Large errors with point source approximation
- Excellent results with $N_h = 7$ heights

Pressure maps in a neutral atmosphere

Difference between extended source model (method 1) and point source approximation for $\tau = 180^o$

Extended source

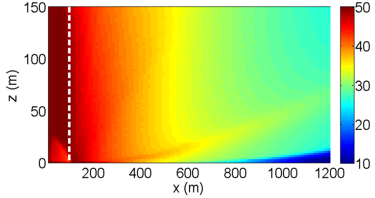

Point source

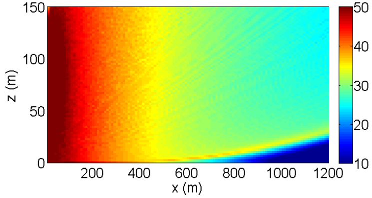

Comparison of both methods in a neutral atmosphere

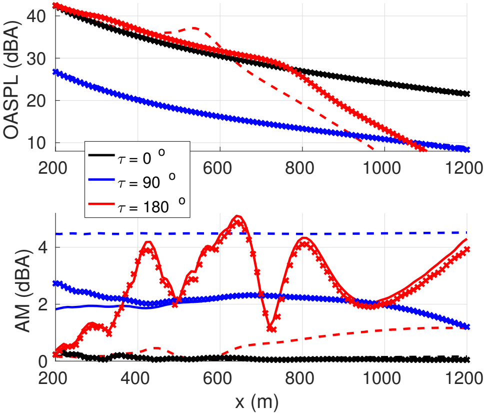

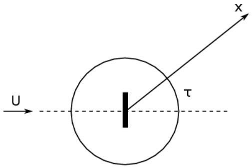

Solid lines: method 1
Dashed lines: point source approximation

Crosses: method 2 with 19 heights

Contribution of TEN and TIN in a neutral atmosphere

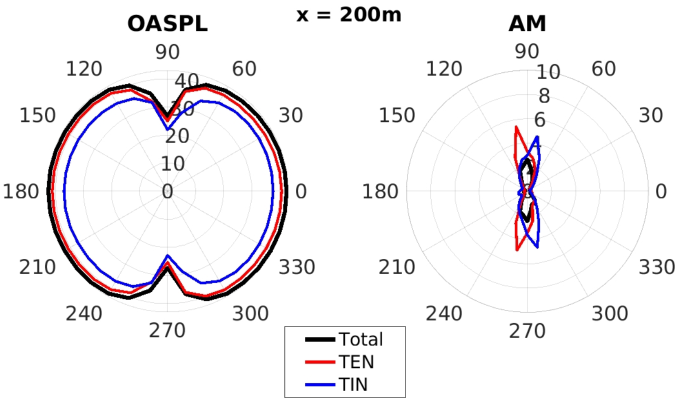

Questions on WTN extended source models?

Outline

Link between atmospheric stability and wind shear

power law profile

$$U(z_2) = U(z_1)\left(\frac{z_2}{z_1}\right)^m$$

shear exponent m

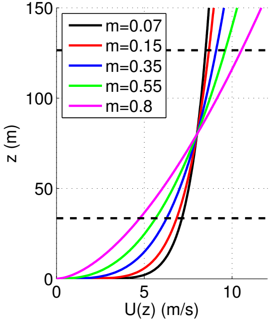

stability class	shear exponent range
unstable	$m \leq 0.1$
(near) neutral	$0.1 < m \leq 0.2$
slightly stable	$0.2 < m \leq 0.4$
very stable	$m > 0.4$

Cabauw site data (van den Berg, 2008)

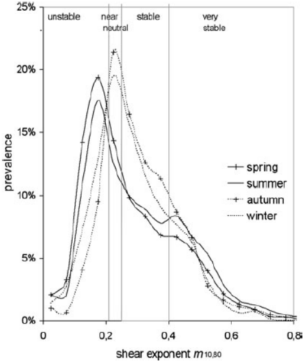

Strong wind shear due to low level jets

- quite common phenomenon in the nocturnal boundary layer
  $\Rightarrow$ typical jet heights between 140 m and 260 m at Cabauw
- related to inertial oscillations around the nocturnal equilibrium wind vector

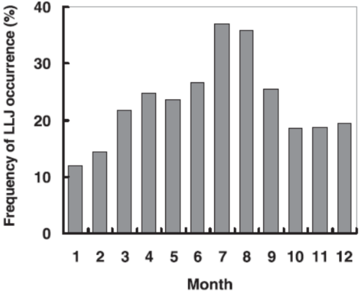

FIG. 5. Frequency of occurrence of LLJ nights per month.

Frequency of occurence of LLJ at Cabauw (Baas *et al.*, 2009)

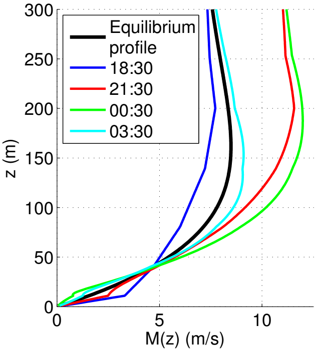

Predictions of van de Wiel *et al.* (2010)

Modeling with Monin-Obukhov similarity theory

- Obukhov length L_* calculated from the sensible heat flux H and the friction velocity u_*:
- Important limitation: MOST valid for $|z/L_*| < 1 - 2$
  $\Rightarrow$ not possible to model strong wind shear situations

Wind speed profiles

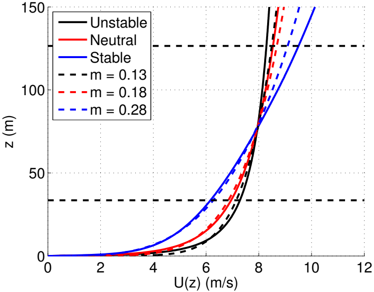

Atmosphere	H (W/m^2)	u_* (m/s)	L_* (m)	$m_{10,80}$
Unstable (U)	200	0.58	-92	0.13
Neutre (N)	0	0.49	∞	0.18
Slightly stable (S)	-25	0.38	200	0.28

Effect of wind shear on wind turbine noise

1. effect on the source emission:
   - higher sound power level than the one predicted from the logarithmically extrapolated 10 m wind ((van den Berg, 2008)
   - AoA variations during one blade rotation ⇒ possible separation/stall noise (Oerlemans, 2013)
2. refraction effects related to wind speed gradients

angle of attack (AoA) variations in degrees for $H = -25\,\mathrm{W/m^2}$ (Tian and Cotté, 2016)

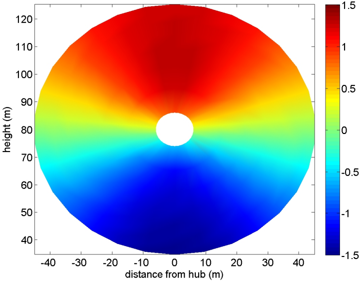

Effect of wind shear on wind turbine noise

Wall pressure spectra Φ_{pp} predicted by Tian and Cotté (2016) for different azimuthal position β

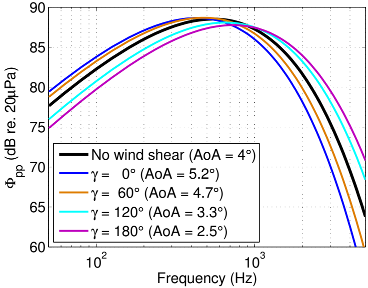

Wall pressure spectra Φ_{pp} measured in the DANAERO project (Madsen *et al.*, 2013)

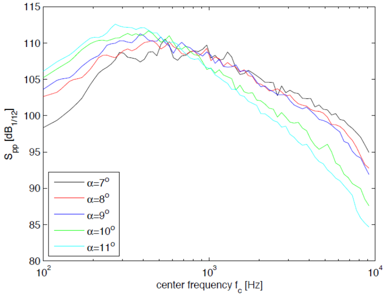

Effect of wind turbine wakes

Main effects of wind turbine wakes:

- velocity deficit behind the WT rotor
- increase of turbulence intensity

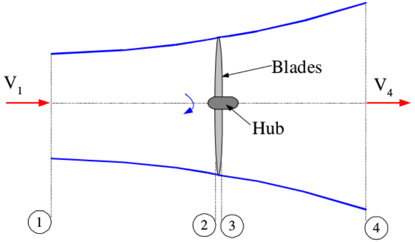

Figure 1: Axial Stream tube around a Wind Turbine

Momentum theory (Ingram, 2011)

Consequences:

- direct: loss of power production !
- indirect: influence acoustic propagation

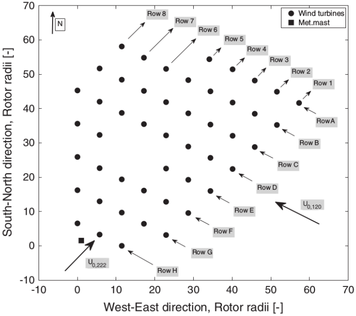

Typical wind farm layout (Nilsson *et al.*, 2015)

Models of wind turbine wakes

- Computational Fluid Dynamics (CFD) simulations of the flow:
  - Reynolds-Averaged Navier-Stokes (RANS) to predict the mean quantities
  - Large Eddy Simulation (LES) to predict the unsteady quantities
- Rotor blades generally represented by equivalent body forces in the momentum equation
  - distributed across the rotor in the Actuator Disk model
  - distributed along the blades in the Actuator Line model

Martinez *et al.* (2012)

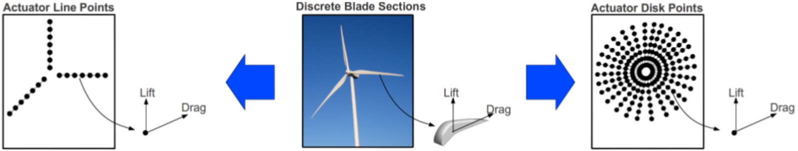

Simulation of wind turbine wakes

Quite accurate predictions of wake development obtained by Sorensen *et al.* (2015) using LES with Actuator Line models for a model wind turbine ($Re = 10^5$)

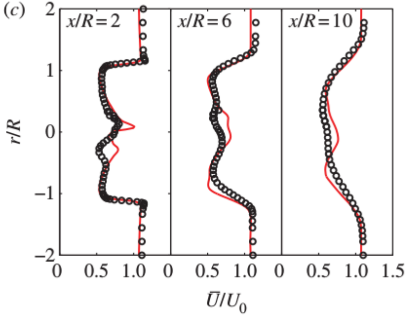

Simulation of wind turbine wakes

Predictions of power production obtained by Nilsson *et al.* (2015) using LES with Actuator Line models

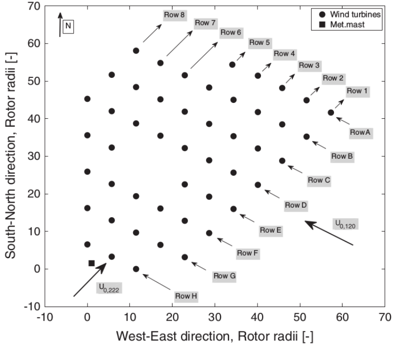

Power production normalized to the front row in the inflow angle sector 120^o and $U_0 = 8\,\mathrm{m/s}$

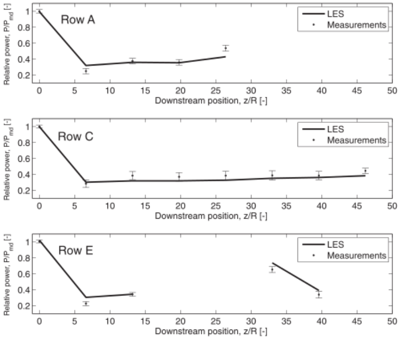

Effect of wind turbine wake on acoustic propagation

Flow simulations of Barlas *et al.* (2017):

- Large Eddy Simulation (LES) with an Actuator Line (AL) technique
- 4 cases with different hub height wind speed (6 or 9 m/s) and surface roughness (0.005 m and 0.5 m).

Effective sound speed profiles $c_{eff} = c + v_x$ with $c = 340$ m/s

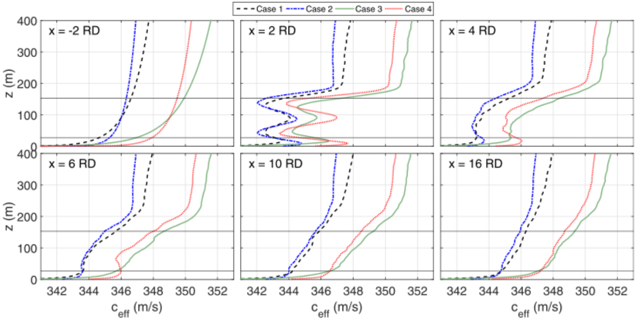

Effect of wind turbine wake on acoustic propagation

Acoustic simulations of Barlas *et al.* (2017):

- Semi-empirical aerodynamic noise source model (NAFNoise)
- 2D PE model for sound propagation with one element per blade between 20 Hz and 800 Hz

Overall SPL at 2m height for flow case 1

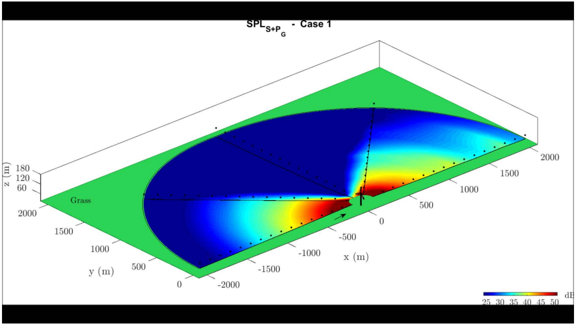

Effect of wind turbine wake on acoustic propagation

Acoustic simulations of Barlas *et al.* (2017):
1/3 octave band spectra downwind (with and without wake) and upwind

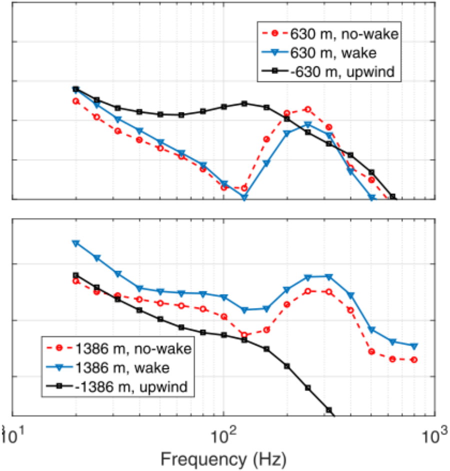

Effect of wind turbine wake on acoustic propagation

Acoustic simulations of Barlas *et al.* (2017):
Amplitude modulation calculated with the source model only (left) and with the propagation effects (right)

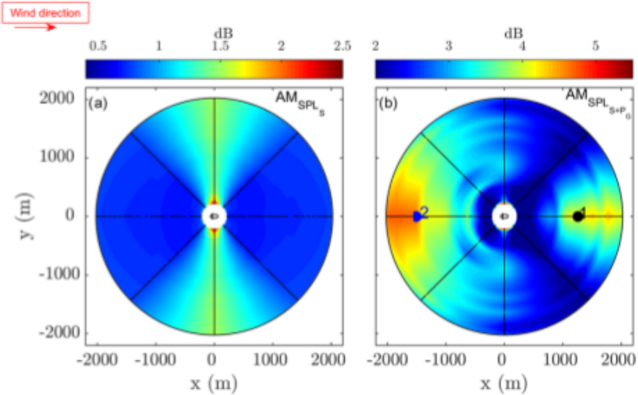

Effect of terrain on flow

- wind turbines commonly placed at top of hills or ridges to benefit from flow speed increase
- speed increase (speed-up):

$$\Delta S = \frac{S(x, \Delta z) - S_0(\Delta z)}{S_0(\Delta z)}$$

with $S = \sqrt{U^2 + V^2 + W^2}$ the velocity magnitude

- turbulent kinetic energy (TKE) increase:

$$\Delta K = \frac{K(x, \Delta z) - K_0(\Delta z)}{K_0(\Delta z)}$$

with $K = \frac{1}{2}\left(\sigma_U^2 + \sigma_V^2 + \sigma_W^2\right)$ the TKE

- detailed experimental campaign: Askervein hill project (1982/1983), Bolund experiment (2007/2008)

LES predictions of Conan *et al.* (2016)

map of ΔS

map of ΔK

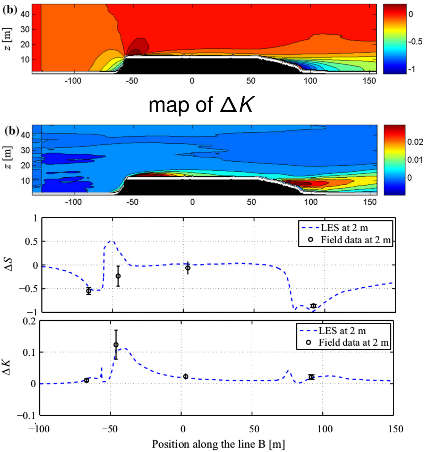

Effect of terrain and wake on acoustic propagation

LES simulations by Heimann *et al.* (2018)

Mean wind speed (A) with WT and without hill (B) with hill and without WT

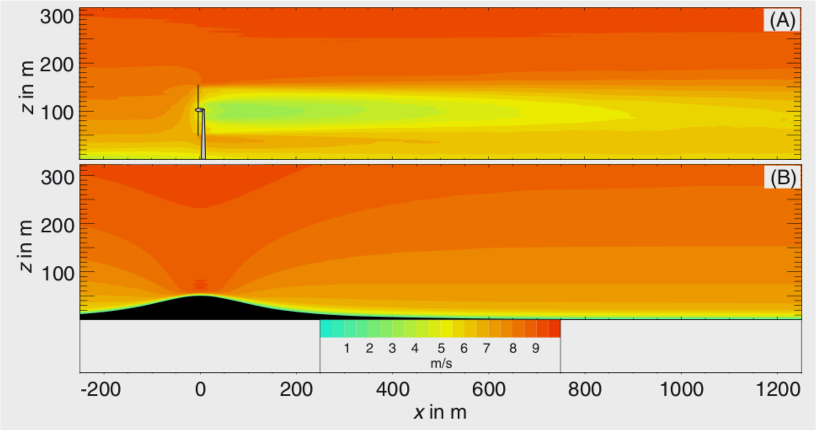

Effect of terrain and wake on acoustic propagation

LES simulations by Heimann *et al.* (2018)

(A)Mean wind speed (B) instantaneous wind speed with WT on top of the hill

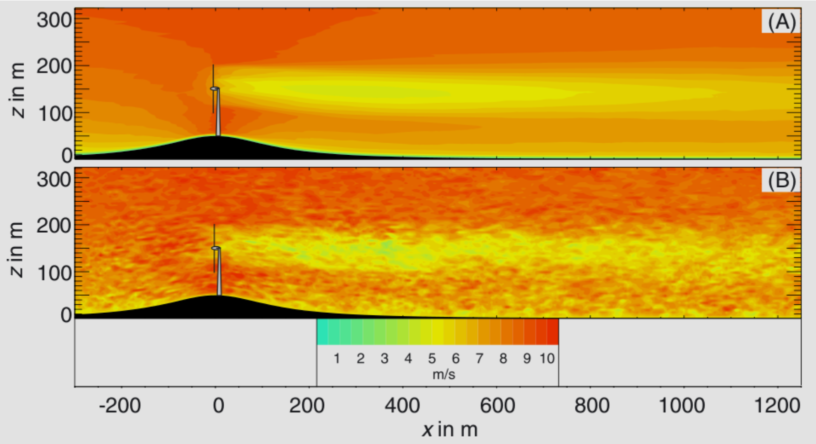

Effect of terrain and wake on acoustic propagation

Acoustic simulations by Heimann *et al.* (2018) using 3D ray-based sound particle model:

- sound reduction of 1-2 dB due to hill effect for distances greater than 6D
- greater amplitude modulation when the hill is present

Near-ground sound level fluctuations without hill (left) and with hill (right)

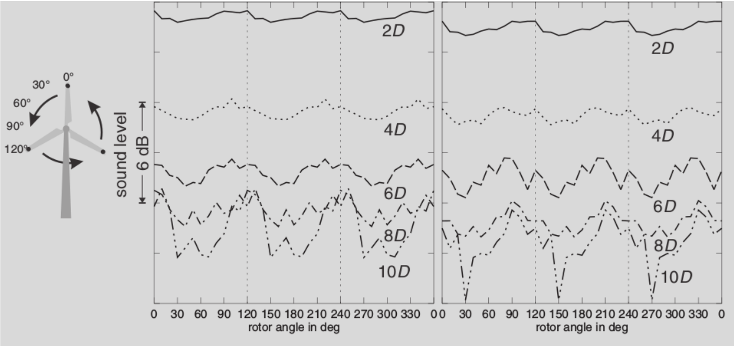

Conclusion and some perspectives

- Wind turbines are complex acoustic sources !
- Be careful when using point source approximation
  $\Rightarrow$ Extended source models needed to get the correct spectra, amplitude modulation, and OASPL upwind
- Important effects of wind shear, wakes and terrain
- Need for *in-situ* experimental validation and study of WTN variability
  $\Rightarrow$ thesis of Bill Kayser directed by Benoit Gauvreau and David Ecotière at UMRAE
- Wind turbine noise sound synthesis
  - synthesis of Pieren *et al.* (2014) based on signal processing techniques
  - EolBF project: physics-based sound synthesis to be used for psychoacoustics tests

Selected bibliography: wind turbine noise generalities

- D. Bowdler and G. Leventhall (2011), Wind Turbine Noise, Multi-Science Publishing.
- I. Old and K. Kaliski (2017), Wind Turbine Noise Dose Response ? Comparison of Recent Studies, 7th International Conference on Wind Turbine Noise, Rotterdam, Netherlands.
- E. Pedersen and K.P. Waye (2014), Perception and annoyance due to wind turbine noise?a dose?response relationship, *J. Acoust. Soc. Am.* **116**, 3460–3470.
- S. Oerlemans (2013), An explanation for enhanced amplitude modulation of wind turbine noise, in "Wind Turbine Amplitude Modulation: Research to Improve Understanding as to its Cause and Effect", Technical report, RenewableUK.
- K.P. Shepherd and H.H. Hubbard (1991), Physical Characteristics and Perception of Low Frequency Noise from Wind Turbines, *Noise Control Eng. J.* **36**, 5–15.
- M. Smith, A. Bullmore, M. Cand and R. Davis (2012), Mechanisms of amplitude modulation in wind turbine noise, Acoustics 2012, Nantes, France.
- B. Zajamsek, K.L. Hansen, C.J. Doolan and C.H. Hansen, Characterisation of wind farm infrasound and low-frequency noise, *J. Sound and Vibration* **370**, 176–190.

Selected bibliography: wind turbine noise sources

- F. Bertagnolio, H.A. Madsen, C. Bak, N. Troldborg, A. Fischer (2015), Aerodynamic Noise Characterization of a Full-Scale Wind Turbine through High-Frequency Surface Pressure Measurements, *Int. J. Aeroacoustics* **14**, 729–766.
- T.F. Brooks, D.S. Pope and M.A. Marcolini, (1989), Airfoil Self-Noise and Prediction, NASA Reference Publication 1218.
- S. Buck, S. Oerlemans and S. Palo (2016), Experimental characterization of turbulent inflow noise on a full-scale wind turbine, *J. Sound and Vibration* **385**, 219–238.
- S. Oerlemans, P. Sijtsma and B. Méndez López (2007), Location and quantification of noise sources on a wind turbine, *J. Sound and Vibration* **299**, 869–883.
- Y. Tian and B. Cotté (2016), Wind turbine noise modeling based on Amiet's theory: Effects of wind shear and atmospheric turbulence, *Acta Acustica United Acustica* **102**, 626–639.
- Y. Yauwenas, B. Zajamsek, J. Reizes, V. Timchenko, and C.J. Doolan (2017), Numerical simulation of blade-passage noise, *J. Acoust. Soc. Am.* **142**, 1575–1586.
- W.J. Zhu, N. Heilskov, W.Z. Shen and J.N. Sørensen (2005), Modeling of Aerodynamically Generated Noise From Wind Turbines, *J. Solar Energy Eng.* **127**, 517–528.

Selected bibliography: extended source models

- E. Barlas, W.J. Zhu, W.Z. Shen, K.O. Dag, and P. Moriarty (2017), Consistent modelling of wind turbine noise propagation from source to receiver, *J. Acoust. Soc. Am.* **142**, 3297–3310.
- B. Cotté (2018), Coupling of an aeroacoustic model and a parabolic equation code for long range wind turbine noise propagation, *J. Sound and Vibration* **422**, 343–357.
- D. Dragna (2011), Modélisation par une approche temporelle de la propagation acoustique en milieu extérieur: traitement de frontières complexes et validation sur site ferroviaire, Ph.D. thesis, École Centrale de Lyon, no. 2011-35.
- K. Heutschi, R. Pieren, M. Müller, M. Manyoky, U.W. Hayek and K. Eggenschwiler (2014), Auralization of Wind Turbine Noise: Propagation Filtering and Vegetation Noise Synthesis, *Acta Acustica United Acustica* **100**, 13–24.
- R. Pieren, K. Heutschi, M. Müller, M. Manyoky, and K. Eggenschwiler (2014), Auralization of Wind Turbine Noise: Emission Synthesis, *Acta Acustica United Acustica* **100**, 25–33.
- J.M. Prospathopoulos and S.G. Voutsinas (2005), Noise Propagation Issues in Wind Energy Applications, *J. Solar Energy Eng.* **127**, 234–241.

Selected bibliography: meteorology, wake and terrain

- P. Baas, F.C. Bosveld, H. Klein, A.A.M. Holstag (2009), A Climatology of Nocturnal Low-Level Jets at Cabauw, *J. Applied Meteorology Climatology* **48**, 1627–1642.
- E. Barlas, W.J. Zhu, W.Z. Shen *et al.* (2017), Consistent modelling of wind turbine noise propagation from source to receiver, *J. Acoust. Soc. Am.* **142**, 3297–3310.
- B. Conan, A. Chaudhari, S. Aubrun *et al.* (2016), Experimental and Numerical Modelling of Flow over Complex Terrain: The Bolund Hill, *Bound. Layer Meteorology* **158**, 183–208.
- D. Heimann, A. Englberger, A. Schady (2018), Sound propagation through the wake flow of a hilltop wind turbine?A numerical study, *Wind Energy*, `https://doi.org/10.1002/we.2185`.
- K. Nilsson, S. Ivanell, K.S. Hansen *et al.* (2015), Large-eddy simulations of the Lillgrund wind farm, *Wind Energy* **18**, 449–467.
- J.N. Sørensen, R.F. Mikkelsen, D.S. Henningson *et al.* and S.J. Andersen (2015), Simulation of wind turbine wakes using the actuator line technique, *Phil. Trans. R. Soc. A* **373**:20140071.
- B.J.H. van de Wiel, A.F. Moene, G.J. Steeneveld *et al.* (2010), A Conceptual View on Inertial Oscillations and Nocturnal Low-Level Jets, *J. Atmospheric Sci.* **67**, 2679–2689.
- G.P. van den Berg (2008), Wind Turbine Power and Sound in Relation to Atmospheric Stability, *Wind Energy* **11**, 151–169.